Atmospheric Pressure Acetylene Detection by UV Photo-Fragmentation and Induced C-2 Emission

Miles, Paul C.; Li, Bo; Li, Zhongshan; Aldén, Marcus

Published in:
Applied Spectroscopy

DOI:
10.1366/12-06731

2013

Atmospheric Pressure Acetylene Detection by UV Photo-Fragmentation and Induced C_2 Emission

Paul C. Miles,[a] Bo Li,[b] Zhongshan Li,[b,*] Marcus Aldén[b]

[a] *Combustion Research Facility, Sandia National Laboratories, P.O. Box 969, MS9053, Livermore, CA 94551-0969, USA*
[b] *Division of Combustion Physics, Lund University, P.O. Box 118, S-221 00 Lund, Sweden*

Detection of C_2H_2 via UV photo-fragmentation, followed by monitoring the C_2 $d^3\Pi_g$–$a^3\Pi_u$ fluorescence, is explored at atmospheric pressure and at temperatures of 295 K, 600 K, and 800 K, for excitation wavelengths 210 to 240 nm using a broadband laser source (~3 cm^{-1} fwhm). At the lower temperature, C_2 emissions correlate closely with C_2H_2 $\tilde{A} \leftarrow X$ absorption bands, and the excitation spectra suggest a higher-transition probability for the $v''_4 = 2$ and 3 states than for the $v''_4 = 0$ and 1 states. As temperature increases, the excitation spectra exhibit a higher nonresonant background.

Index Headings: **Ultraviolet Photo-fragmentation; Acetylene detection; C_2 Swan band; Fluorescence.**

INTRODUCTION

Acetylene (C_2H_2) is an important intermediate species in hydrocarbon combustion and a key species for soot formation and growth. Moreover, together with CH_4 and C_2H_4, it is one of the dominant hydrocarbon (HC) species found in the partial oxidation products of moderately rich mixtures. Figure 1 shows the makeup of the unburned hydrocarbons (UHC) predicted for the combustion of a homogeneous mixture of *n*-C_7H_{16} in an environment typical of a reciprocating engine. All other HC species are present in quantities of less than 1 ppm. Clearly, a method of detecting C_2H_2 would be useful for detecting in-cylinder sources of UHC emissions associated with overly rich mixtures in engines, as well as for evaluating the effectiveness of the mixing processes in a variety of other practical combustion devices. Moreover, if such a detection technique were to be made quantitative, it would be very useful for the validation of chemical kinetic models of hydrocarbon combustion and for developing and validating models for soot formation.

Several techniques have been developed for C_2H_2 detection in flames, e.g., mass spectroscopy of sampled gases (MS),[1] coherent anti-Stokes Raman scattering (CARS),[2] mid-infrared polarization spectroscopy (mid-IRPS),[3] and tunable diode laser absorption spectroscopy (TDLAS).[4] The MS technique suffers from intrusiveness, the CARS and IRPS methods are complex and can suffer from inadequate spatial resolution, and the TDLAS technique provides only line-of-sight information. In contrast, UV photo-fragmentation offers the potential for spatially resolved, planar detection of C_2H_2 using a single laser and inexpensive signal detection optics and cameras. Raiche et al.[5] have shown that C_2H_2 can be detected in low-pressure flames by monitoring C_2 fluorescence with the excitation laser tuned to a known C_2H_2 absorption line. However, nonresonant wavelengths also produced C_2 emissions, indicating potential interference from other species. Recently, Osborne and Frank[6] have explored the possibility that Swan band fluorescence of C_2 observed in CO-imaging studies of methane/air flames is associated with the photo-fragmentation of C_2H_2 to produce excited C_2. Similar fluorescent interference has been observed in CO measurements in engines.[7] Osborne and Frank[6] evaluated seven prospective C_2 precursor molecules, including C_2H_2, CH_4, and C_2H_4—the three hydrocarbon species dominating the partial-oxidation products shown in Fig. 1. Of these three species, only C_2H_2 produced significant Swan band emissions. Consequently, the likelihood of significant interference from other hydrocarbon species in the products of moderately rich combustion is small. Like the work of Raiche et al.,[5] the Osborne and Frank[6] experiments were performed at low pressure (5 Torr). The experiments described in the present work are aimed at determining whether laser-induced photo-fragmentation can potentially serve as a viable diagnostic for high-pressure detection of C_2H_2—appropriate to the pressures and temperatures characteristic of practical combustion devices, such as reciprocating engines or gas turbine combustors.

BACKGROUND

In its ground state, C_2H_2 is a linear molecule characterized by five distinct normal vibrational modes: v_1, symmetric C–H stretch; v_2, symmetric C–C stretch; v_3, asymmetric C–H stretch; v_4, *trans*-bending; and v_5, *cis*-bending. The two bending modes are doubly degenerate and have associated angular momentum quantum numbers l_4 and l_5. In the $\tilde{A}$ state,

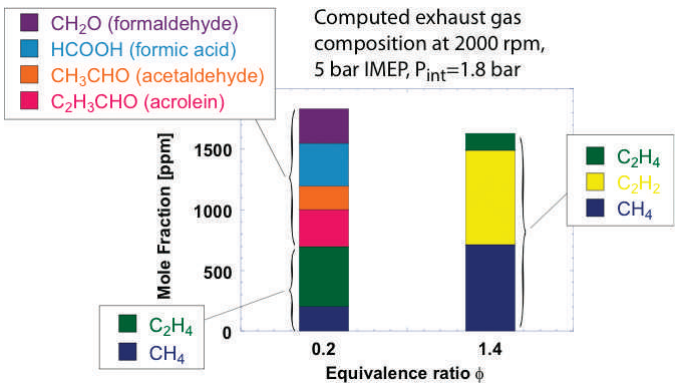

FIG. 1. Acetylene is a dominant component of the unburned hydrocarbon emissions stemming from rich mixtures. Unlike the emissions from lean mixtures, none of the rich-mixture species are readily accessible with laser-based diagnostic techniques.

Received 15 May 2012; accepted 21 September 2012.
* Author to whom correspondence should be sent. E-mail: zhongshan.li@forbrf.lth.se
DOI: 10.1366/12-06731

0003-7028/13/6701-0066/0

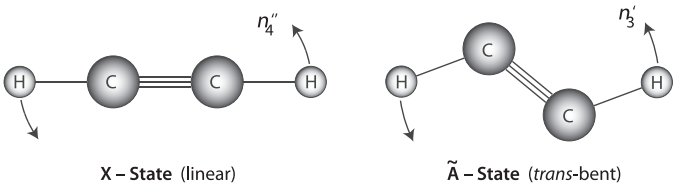

FIG. 2. Schematic diagram of the X and Ã states of C_2H_2 and their corresponding *trans*-bending vibrational modes.

C_2H_2 has a *trans*-bent, planar structure and, thus, has one fewer vibrational modes. In this case, the modes are numbered differently, with v_3 corresponding to the *trans*-bending mode. Because of the similarity in nuclear positions between the X-state *trans*-bending mode shown in Fig. 2 and the *trans*-bent Ã state, one can expect, on Franck-Condon grounds, that Ã–X transitions will be dominated by v'_3–v''_4 vibrational transitions. This expectation is borne out by measured UV absorption spectra.[8,9]

Rapid rise times in the intensity of C_2 Swan $d^3\Pi_g$–$a^3\Pi_u$ emissions observed in low pressure C_2H_2 photo-fragmentation experiments[5,10] imply that the C_2 fragments are unimolecular dissociation products formed during the laser pulse. These fragments are believed to form via a three-photon process,[5,6,10] commencing with an initial absorption to the Ã state, followed by a second absorption and rapid dissociation to create highly excited $C_2H + H$. Absorption of a third photon then yields C_2 ($d^3\Pi_g$) + H + H. Based on energy considerations, it is not possible to form C_2 ($d^3\Pi_g$) from C_2H_2 (X) with only two photons for excitation wavelengths longer than ~185 nm. However, multiple three-photon paths to the final product species, with differing photometric efficiencies, may exist. For example, considering that the dissociation energy D_0 of C_2H_2 (X), yielding C_2H ($\tilde{X}$) + H, is ~46 070 cm^{-1},[11] we anticipate that C_2H ($\tilde{X}$) can be formed by a single absorption, with excitation wavelengths shorter than ~217 nm. Indeed, C_2H_2 Ã → X emission intensity has been observed to drop dramatically for excitation wavelengths below ~216 nm,[12] even though the absorption continues to increase with decreasing wavelength. Subsequent, two-photon processes taking C_2H ($\tilde{X}$) to C_2 ($d^3\Pi_g$) + H might lead to overall process efficiencies that differ significantly from processes requiring an initial two-photon absorption. Accordingly, one objective of this work was to explore the effect of excitation wavelength on the C_2 fluorescence intensity.

In a similar vein, we anticipate that vibrationally excited C_2H_2 may have advantageous Franck–Condon overlap factors with the Ã state, and hence, could exhibit differing photometric efficiency in the formation of C_2 ($d^3\Pi_g$). This possibility is supported by vibrationally mediated photodissociation studies,[13] which have shown that vibrationally excited C_2H_2 (X) preferentially yields C_2H (Ã), whereas direct single-photon excitation of the ground state C_2H_2 yields products dominated by C_2H ($\tilde{X}$), even though the total excitation energies differ by only 1220 cm^{-1}. Moreover, with sufficient vibrational excitation ($v'_1 + v'_3 \geq 4$, say), it is energetically feasible to form C_2 ($d^3\Pi_g$) with only two photons at laser wavelengths accessible with inexpensive, commercial optical parametric oscillators (OPOs). In this work, we, consequently, also examine the effect of temperature on the C_2 excitation spectrum to ascertain whether advantageous single-wavelength excitation strategies exist to detect thermally excited C_2H_2.

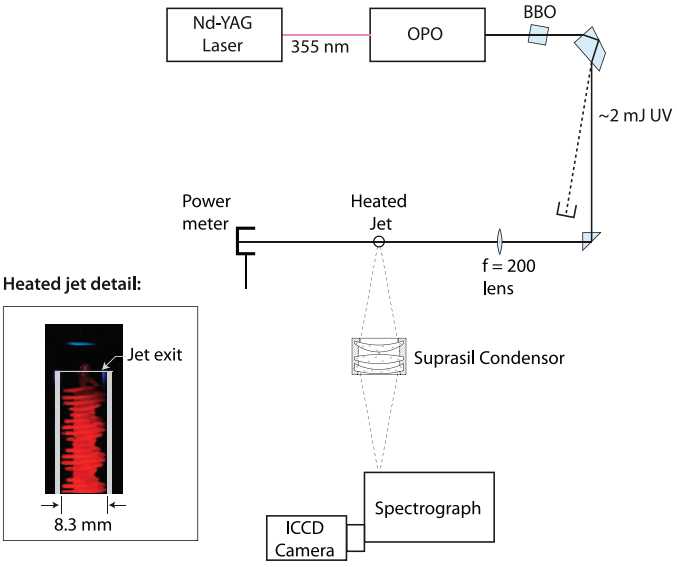

FIG. 3. Schematic diagram of the experimental configuration and details of the heated jet.

EXPERIMENT

The experimental configuration is shown in Fig. 3. The third harmonic (355 nm) of a Nd : YAG (neodymium-doped yttrium aluminum garnet) laser (Spectra-Physics, PRO-290) was used to pump an OPO system (GWU Premi-Scan/MB). The output from the OPO was frequency-doubled in a β-barium borate (BBO) crystal, and a UV beam was achieved within a tunable wavelength range of 210–242 nm. The UV beam was focused by a spherical lens ($f = 200$ mm) approximately 5 mm above the exit of a quartz tube heater (OSRAM SYLVANIA, series I-014372) with an inner diameter of 0.83 cm and a length of 19.7 cm. The gas is supplied from the bottom of the tube and heated by a coiled ferrous alloy filament as it passes through the tube. By tuning the gas supply speed and the voltage on the heating wire, we controlled the temperature of the gas jet at the exit of the tube. The estimated residence time of the gas within the tube was less than 1 s.

Excitation scans were performed between 210–242 nm. The C_2 fluorescence was collected by a 70 mm focal-length UV quartz condenser and focused into an *f*/4 spectrograph (Acton 2300i, grating: 300 g/mm, blazed at 300 nm), which provided a dispersion of 10.6 nm/mm in the exit plane. The spectrally dispersed emissions were recorded by an ICCD (intensified charge-coupled device) camera (Princeton PI MAX 2, 1024 × 1024). With a 13.1 × 13.1 mm camera detector area and a slit width of 0.25 mm, the recorded spectra had a bandwidth of approximately 140 nm and a resolution of 2.6 nm. The measured intensifier gate width was 110 ns and was phased to collect both prompt and delayed emissions. At each excitation wavelength, emission spectra were collected and averaged over 1000 laser pulses. Each excitation scan was performed at a constant average laser pulse energy, which was held at a fixed level of ~2 mJ. The corresponding irradiance level near the beam focus was approximately 5×10^8 W/cm^2. Under these

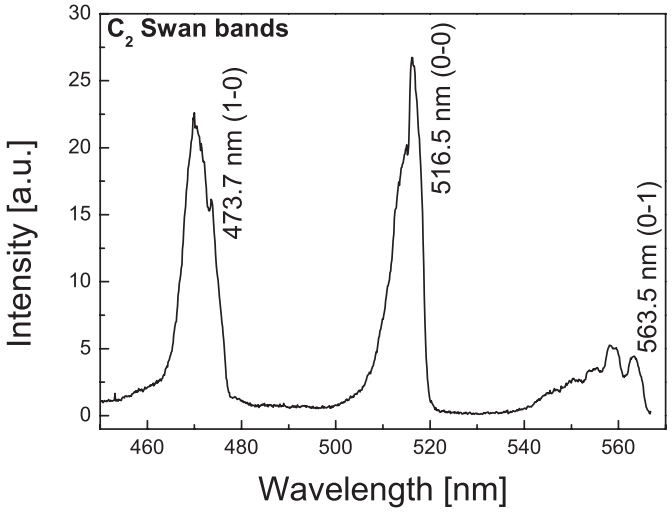

FIG. 4. Emission spectrum of photo-fragmented C_2 near the heated jet at a temperature of 800 K. The middle bands (519.8–508.0 nm) were collected at each excitation wavelength.

conditions, with the laser tuned to a C_2H_2 absorption band, the blue-green Swan band emissions were readily visible to the naked eye.

The measured spectrum of C_2 $d^3\Pi_g$–$a^3\Pi_u$ (Swan) emissions is shown in Fig. 4. The center wavelength of the spectrograph was set to 498 nm, such that Swan emissions from the $\Delta v = 0$ and $\Delta v = \pm 1$ bands were visible. Average signal levels were determined by integrating the signal over the $\Delta v = 0$ band from 19 240–19 680 cm^{-1} (519.8–508.0 nm; see Fig. 4) and subtracting a background level determined by integrating over the adjacent, equal pixel-width region, where no signal was observed (18 810–19 240 cm^{-1}, or 531.6–519.8 nm). Figure 4 shows that only C_2 Swan band emissions were detected in this spectral region.

Low-resolution excitation scans were performed at a fixed wavenumber increment of 100 cm^{-1} (50 cm^{-1} near known strong C_2H_2 absorption bands) and were followed by more-moderate resolution (20 cm^{-1}) scans to clarify the structure of absorbing regions identified in the low-resolution scans. The OPO line width, before doubling, is specified to be 3–6 cm^{-1} fwhm. The specification was verified with a Yokogawa model AQ6375 optical spectrum analyzer. The accuracy of the OPO wavelength setting was verified to be better than 2 cm^{-1} by comparing with emission lines from a mercury calibration lamp. The laser irradiance dependency of several peaks in the excitation spectrum was also examined by varying the laser energy.

The excitation scans were performed at temperatures of 295 K, 600 K, and 800 K in the jet exiting the tube heater. The jet fluid was delivered from a gas cylinder prepared by Matheson Tri-Gas Inc. to have 2% C_2H_2 in N_2. No additional purification or conditioning of the cylinder gas was performed. Jet exit temperatures were measured with a 0.08 mm wire diameter, type R thermocouple, and were maintained within ±10 K of the set point.

RESULTS

A low-resolution fluorescence excitation scan obtained within the jet at ambient pressure and temperature is shown in Fig. 5. Although the C_2 emissions are greatest when the photon energy is greater than the C_2H–H bond energy D_0, the emissions rise steadily as the laser wavelength decreases, and there is no obvious discontinuity that occurs at D_0. Rising signal levels could be associated with increased efficiency in either absorption or dissociation processes at higher energies; similar behavior[14] observed between 47 000 and 50 600 cm^{-1} in studies of C_2H_2 dissociation as detected by H atom REMPI (resonance-enhanced multiphoton ionization) has been attributed to more efficient dissociation.

A moderate-resolution scan of wavelengths with photon energies greater than D_0 was also performed to highlight the structure in this region and to search for any emissions peaks that might have been missed with the 50–100 cm^{-1} scan resolution in Fig. 5. The results are shown in Fig. 6a, which also shows the locations of strong C_2H_2 absorption band origins.[8,9] Likewise, band origins for photon energies less than D_0 are shown in Fig. 6b, which reproduces the spectrum of Fig. 5, employing a log scale to better identify bands with low C_2 emission intensities. The band origins are labeled following the notation in Watson et al.[8] and Van Craen et al.,[9] wherein the symbol V_n^m denotes the transition mv'_3–nv''_4, and the symbol K_i^j denotes the transition iK'_a–jl''_4, with K'_a being the axial angular momentum quantum number in the $\tilde{A}$ state.

The spectra shown in Fig. 6 indicate that the C_2 Swan emissions were closely correlated with the C_2H_2 $\tilde{A} \leftarrow X$ absorption probabilities, indicating that more-efficient dissociation with increasing photon energy likely plays a minor role in enhancing the signal levels. Peaks in emission intensity were well represented by the V_n^m band origins, and the magnitude of the peaks is generally highest for $\Delta K = \pm 1$, as is the absorption probability. A few peaks, notably the one near 46 800 cm^{-1} in Fig. 6a and the one near 44 000 cm^{-1} in Fig. 6b, do not correspond to strong C_2H_2 absorption lines. However, those peaks are relatively minor and appear to be of little diagnostic utility.

Although the energy considerations discussed earlier indicate that the production of C_2 ($d^3\Pi_g$) from ground state C_2H_2 will require three photons, it is nevertheless of interest to examine the laser irradiance dependency of the more promising

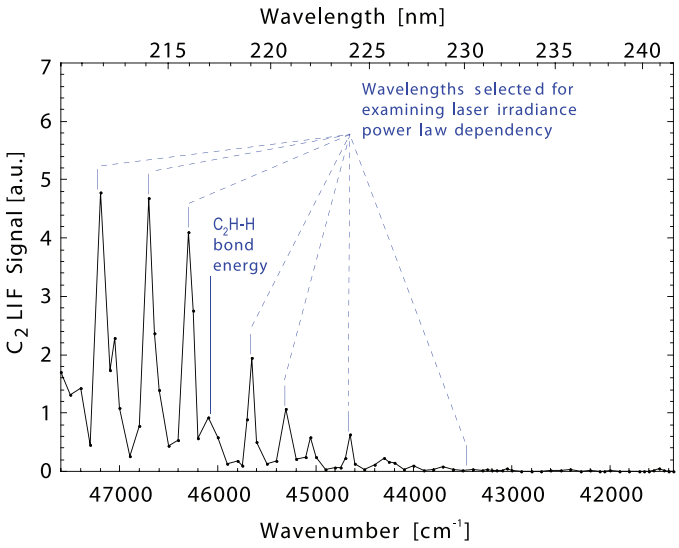

FIG. 5. Low-resolution excitation spectrum of C_2 Swan band emissions in a 295 K jet of 2% C_2H_2 in N_2 at a pressure of 1 atm.

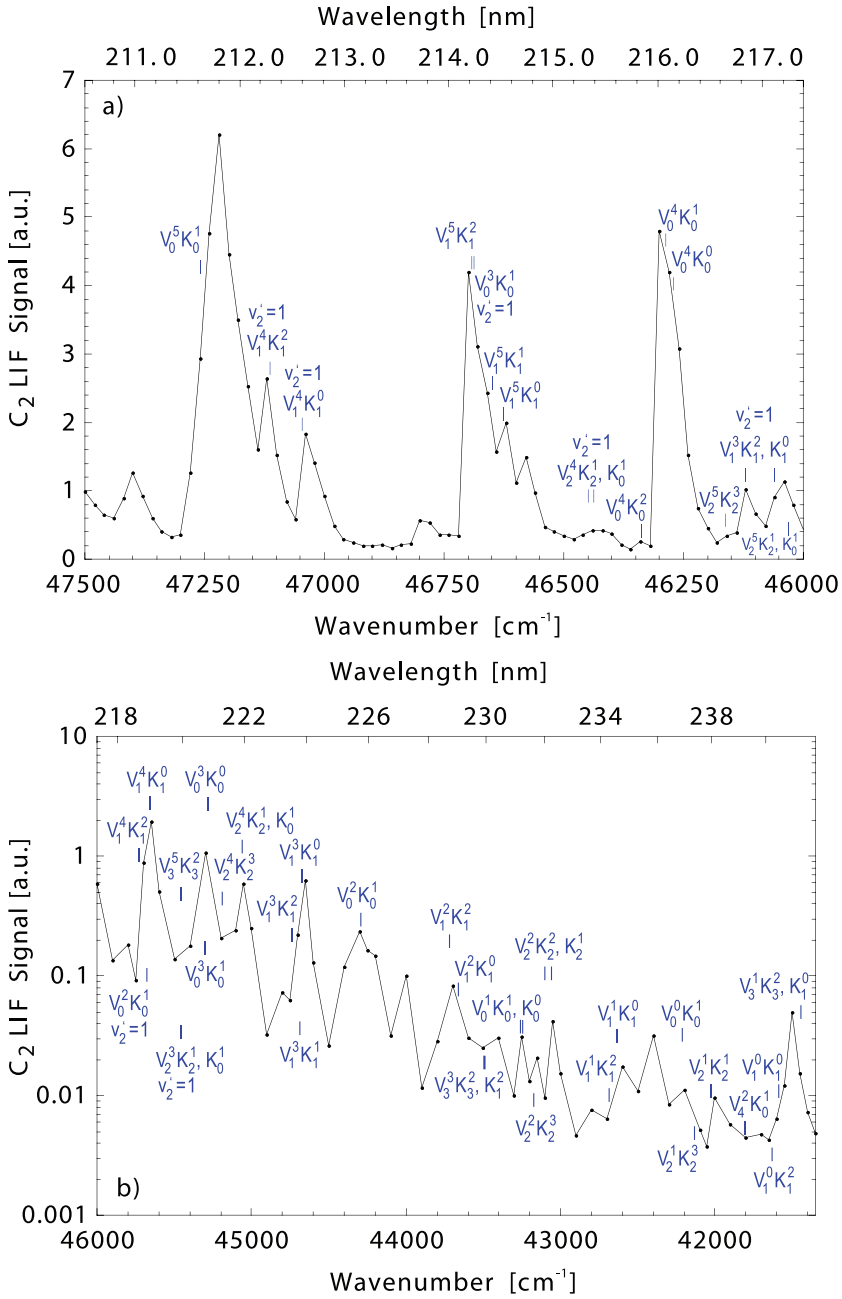

FIG. 6. (**a**) Moderate (20 cm^{-1}) resolution scan for excitation energies greater than D_0; (**b**) labeled transitions within the low-energy portion of the spectrum of Fig. 5.

transitions. Experiments varying the laser irradiance were conducted at each of the six most prominent peaks in the spectrum of Fig. 5, as well as at 230.1 nm, corresponding to the excitation wavelength for CO B ← X (0,0) transitions. Before conducting each laser irradiance sweep, the laser frequency was set to provide the local peak signal intensity by conducting a search with a resolution of 10 cm^{-1}. The results are shown in Fig. 7.

In general, the laser irradiance exponents lie between 2.1 and 3.1. A measure of the uncertainty in the exponent, ±0.3, was obtained by finding the change in the exponent required to reduce the power-law fit correlation coefficient from an average value of 0.995 to 0.990. Within that uncertainty, the measured exponents are consistent with creation of C_2 via a three-photon process. As can be seen, there is a tendency toward lower exponents at longer wavelengths. This suggests that the path followed in the creation of C_2 (or one of multiple paths) at longer wavelengths is either rate-limited by two-photon processes or involves a step whereby irradiance-dependent loss mechanisms, such as photo-ionization, saturation, or stimulated emission, are not insignificant.

The structure of the C_2H_2 excitation spectrum changes significantly at higher jet temperatures, as shown in Figs. 8a and 8b. To compare relative signal intensities as closely as possible, the signals obtained at the higher jet temperatures have been scaled by temperature, which is inversely propor-

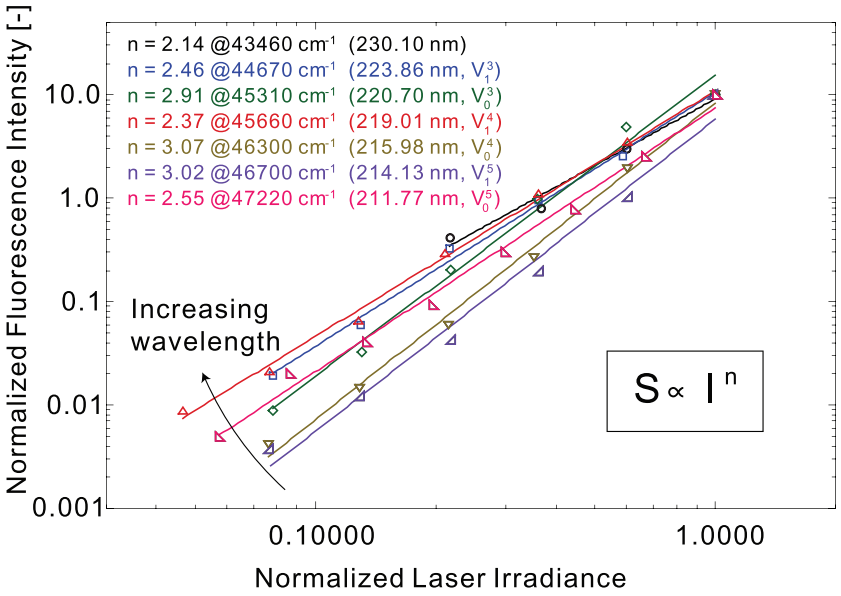

FIG. 7. Laser irradiance dependency of the C_2 emission intensity. The scales are normalized by the highest achievable irradiance at each wavelength and the corresponding signal level.

tional to the relative C_2H_2 number density at the jet exit. In addition to the strong absorption bands identified in Watson et al.[8] and Van Craen et al.,[9] medium and weak bands that correlate closely with dominant features of the C_2H_2 excitation spectrum are also identified (in red) in Fig. 8.

At elevated temperature, significant C_2 emissions are observed at excitation wavelengths that are nonresonant with C_2H_2 $\tilde{A}$–X transitions—with the nonresonant signal strength rising at shorter wavelengths. At resonant wavelengths, however, the peak C_2 emissions are comparable to those seen in Fig. 5. The overall shape of the low-resolution spectrum in Fig. 8a suggests that, with increasing temperature, the central portion of the spectrum (46 000–44 000 cm^{-1}) is enhanced relative to the higher energy portion that dominated Fig. 5. Examination of the particular vibrational transitions involved indicates that this is likely due to the decreased population of the $v''_4 = 0$ and 1 states, characterizing excitation wavenumbers >46 000 cm^{-1}, relative to the $v''_4 = 2$ and 3 states, which are more prevalent in the central portion of the spectrum. The higher-resolution spectrum, in particular, further suggests that the transition probabilities for the $v''_4 = 2$ and 3 states are greater than the probabilities for the $v''_4 = 0$ and 1 states. This observation seems physically plausible because the higher-energy vibrations are more likely to achieve nuclear positions that match the positions of the *trans*-bent $\tilde{A}$ state more closely.

SUMMARY AND CONCLUSIONS

The detection of C_2H_2 via UV photo-fragmentation, monitoring C_2 $d^3\Pi_g$–$a^3\Pi_u$ fluorescence, is explored at atmospheric pressure and at temperatures of 295 K, 600 K, and 800 K. Excitation spectra from 210–240 nm and signal dependencies on laser irradiance support the following conclusions:

1. C_2 laser-induced fluorescence (LIF) emissions increase steadily as the laser wavelength decreases, but there is no obvious discontinuity that occurs when photon energies fall below D_0 (C_2H–H).
2. C_2 emissions correlate closely with the C_2H_2 $\tilde{A} \leftarrow X$ absorption probability, indicating that changes in the efficiency of the dissociation processes ($C_2H_2 \rightarrow C_2H + H$ or $C_2H \rightarrow C_2 + H$) play a minor role in enhancing signal levels.
3. The dependency of C_2 emissions on irradiance fits well with a power law, with exponents between 2.1 and 3.1 ± 0.3, indicating that the absorption–dissociation path followed may be rate-limited by a two-photon processes or subject to irradiance-dependent loss mechanisms, such as photo-ionization, saturation, or stimulated emission.
4. At elevated temperatures, significant C_2 emissions are observed at excitation wavelengths that are nonresonant with C_2H_2 $\tilde{A}$–X transitions.
5. Higher C_2 emissions at excitation wavelengths that correspond to C_2H_2 X ($v''_4 = 2, 3$) transitions, rather than $v''_4 = 0, 1$ transitions, indicate that transitions originating in *trans*-bent excited states of C_2H_2 have a greater probability to produce the C_2 *d* state.

Although resonant excitation near the V_0^5, V_1^4,V_1^5, and V_0^4 bands at wavelengths less than ~216 nm is advantageous for detection of at C_2H_2 via photo-fragmentation at 295 K, at higher temperatures, that advantage is rapidly lost because of the higher C_2 emissions observed when *trans*-bent initial states of C_2H_2 are excited (e.g., V_0^5 near 222 nm). Despite rising C_2 emissions for nonresonant excitation at higher temperatures, resonant excitation still provides up to a two-fold signal-level improvement over nonresonant excitation at temperatures up to 800 K. The high C_2 Swan-band emissions observed with nonresonant excitation do not rule out photo-fragmentation as a viable C_2H_2 diagnostic technique; nevertheless, they indicate that fluorescent emissions from various C_2 systems will be a potential source of interference for a number of combustion diagnostics when C_2H_2 is present. The present work has focused entirely on the excitation characteristics of C_2H_2 photo-fragmentation. Additional work at higher temperatures and pressures, characterization the C_2 emission intensity variation as a function of C_2H_2 concentration, and evaluation

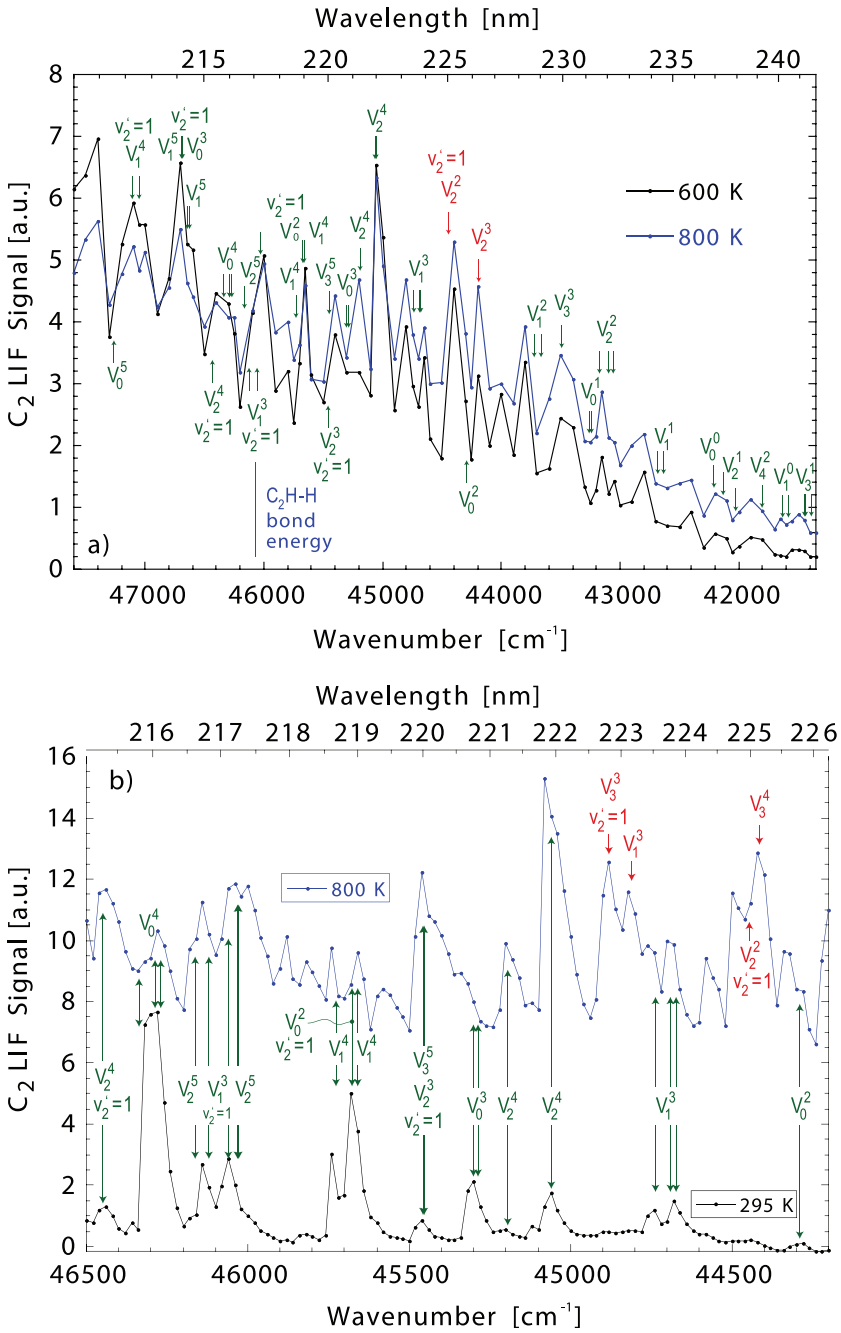

FIG. 8. (**a**) Low-resolution C_2 excitation spectra in the heated jet; (**b**) moderate (20 cm^{-1}) resolution spectra focusing on the dominant transitions observed at elevated temperature. More laser energy was available in (**b**) because of the reduced scan bandwidth.

of potential C_2 generation from other common combustion species at elevated temperatures and pressures is still required before C_2H_2 photo-fragmentation can be regarded as a useful diagnostic tool.

ACKNOWLEDGMENTS

This work was performed at the Department of Combustion Physics at Lund University and at the Combustion Research Facility of Sandia National Laboratories. The authors gratefully acknowledge Scania AB for financial support for this work; Joakim Bood and David Osborn for helpful technical discussions; and Öivind Andersson and Bengt Johansson of the Lund University Department of Energy Sciences for facilitating this collaboration. The Lund University authors acknowledge CECOST (through the Energy Agency and the Foundation for Strategic Research, SSF) and ERC (through the Advanced Grant 'DALDECS') for financial support. Sandia is a multi-program laboratory operated by Sandia Corporation, a Lockheed Martin Company, for the United States Department of Energy's National Nuclear Security Administration under contract DE-AC04-94AL85000.

1. B. Atkana, A.T. Hartlieb, J. Brand, K. Kohse-Höinghaus. "An Experimental Investigation of Premixed Fuel-Rich Lowpressure Propene/Oxygen/Argon Flames by Laser Spectroscopy and Molecular-Beam Mass Spectrometry". Proc. Combust. Inst. 1998. 27(2): 435-444.
2. R.L. Farrow, R.P. Lucht, W.L. Flower, R.E. Palmer. "Coherent Anti-Stokes Raman Spectroscopic Measurements of Temperature and Acetylene Spectra in a Sooting Diffusion Flame: Colloquium on Combustion Diagnostics". Proc. Combust. Inst. 1985. 20(1): 1307-1312.
3. Z.W. Sun, Z.S. Li, B. Li, Z.T. Alwahabi, M. Aldén. "Quantitative C_2H_2 Measurements in Sooty Flames using Mid-Infrared Polarization Spectroscopy". Appl. Phys. B, Lasers Opt. 2010. 101(1): 423-432.

4. S. Wagner, B.T. Fisher, J.W. Fleming, V. Ebert. "TDLAS-Based In Situ Measurement of Absolute Acetylene Concentrations in Laminar 2D Diffusion Flames". Proc. Combust. Inst. 2009. 32(1): 839-846.
5. G.A. Raiche, D.R. Crosley, R.A. Copeland. "Laser-Induced Fluorescence and Dissociation of Acetylene in Flames". Paper presented at: Advances in Laser Science IV, American Institute of Physics Conference Proceedings. Atlanta, GA; 1989. 191: 758-760.
6. D.L. Osborn, J.H. Frank. "Laser-Induced Fragmentation Fluorescence Detection of the Vinyl Radical and Acetylene". Chem. Phys. Lett. 2001. 349: 43-50.
7. D. Kim, I. Ekoto, W.F. Colban, P.C. Miles. "In-Cylinder CO and UHC Imaging in a Light-Duty Diesel Engine During PPCI Low-Temperature Combustion". SAE Int. J. Fuels Lubr. 2009. 1: 933-956.
8. J.K.G. Watson, M. Herman, J.C. Van Craen, R. Colin. "The A–X Band System of Acetylene". J. Mol. Spectrosc. 1982. 95: 101-132.
9. J.C. Van Craen, M. Herman, R. Colin, J.K.G. Watson. "The A–X Band System of Acetylene: Analysis of Medium-Wavelength Bands, and Vibration-Rotation Constants for the Levels nv'_3 ($n = 4$–6), $v''_2 + nv'_3$ ($n = 3$–5), and $v'_1 + nv''_3$ ($n = 2, 3$)." J. Mol. Spectrosc. 1985. 111: 185-197.
10. J.R. McDonald, A.P. Baronavski, V.M. Donnelly. "Multiphoton-Vacuum-Ultraviolet Laser Photodissociation of Acetylene: Emission from Electronically Excited Fragments". Chem. Phys. 1978. 33: 161-170.
11. D.H. Mordaunt, M.N.R. Ashfold. "Near-Ultraviolet Photolysis of C_2H_2: A Precise Determination of D_0(HCC–H)". J. Chem. Phys. 1994. 101: 2630-2631.
12. M. Fujii, A. Haijima, M. Ito. "Predissociation of Acetylene in the $\tilde{A}^1$ A_u State". Chem. Phys. Lett. 1988. 150: 380-385.
13. J. Zhang, C.W. Riehn, M. Dulligan, C. Wittig. "Propensities Toward $C_2H(\tilde{A}^2\ \Pi)$ in Acetylene Photodissociation". J. Chem. Phys. 1995. 103: 6815-6818.
14. N. Yamakita, S. Iwamoto, S. Tsuchiya. "Predissociation of Excited Acetylene in the $\tilde{A}^1$ A_u State Around the Adiabatic Dissociation Threshold as Studied by LIF and H-Atom Action Spectroscopy". J. Phys. Chem. A. 2003. 107: 2597-2605.